We are IntechOpen,
the world's leading publisher of
Open Access books
Built by scientists, for scientists

4,800
Open access books available

122,000
International authors and editors

135M
Downloads

Our authors are among the

154
Countries delivered to

TOP 1%
most cited scientists

12.2%
Contributors from top 500 universities

WEB OF SCIENCE™

Selection of our books indexed in the Book Citation Index
in Web of Science™ Core Collection (BKCI)

Interested in publishing with us?
Contact book.department@intechopen.com

Numbers displayed above are based on latest data collected.
For more information visit www.intechopen.com

Optical Resonators and Dynamic Maps

V. Aboites, Y. Barmenkov, A. Kir'yanov and M. Wilson

Additional information is available at the end of the chapter

http://dx.doi.org/10.5772/51854

1. Introduction

In recent years, optical phase conjugation (OPC) has been an important research subject in the field of lasers and nonlinear optics. OPC defines a link between two coherent optical beams propagating in opposite directions with reversed wave front and identical transverse amplitude distributions. The distinctive characteristic of a pair of phase-conjugate beams is that the aberration influence imposed on the forward beam passed through an inhomogeneous or disturbing medium can be automatically removed for the backward beam passed through the same disturbing medium. There are three main approaches that are efficiently able to produce the backward phase-conjugate beam. The first one is based on the degenerate (or partially degenerate) four-wave mixing processes (FWM), the second is based on a variety of backward simulated (e.g. Brillouin, Raman or Kerr) scattering processes, and the third is based on one-photon or multi-photon pumped backward stimulated emission (lasing) processes. Among these different approaches, there is a common physical mechanism in generating a backward phase-conjugate beam, which is the formation of the induced holographic grating and the subsequent wave-front restoration via a backward reading beam. In most experimental studies, certain types of resonance enhancements of induced refractive-index changes are desirable for obtaining higher grating-refraction efficiency. OPC-associated techniques can be effectively utilized in many different application areas: such as high-brightness laser oscillator/amplifier systems, cavity-less lasing devices, laser target-aiming systems, aberration correction for coherent-light transmission and reflection through disturbing media, long distance optical fiber communications with ultra-high bit-rate, optical phase locking and coupling systems, and novel optical data storage and processing systems (see Ref. [1] and references therein).

The power performance of a phase conjugated laser oscillator can be significantly improved introducing intracavity nonlinear elements, e.g. Eichler et al. [2] and O'Connor et al. [3] showed that a stimulated-Brillouin-scattering (SBS) phase conjugating cell placed inside the resonator of a solid-state laser reduces its optical coherence length, because each axial mode

of the phase conjugated oscillator experiences a frequency shift at every reflection by the SBS cell resulting in a multi-frequency lasing spectrum, that makes the laser insensitive to changing operating conditions such as pulse repetition frequency, pump energy, etc. This ability is very important for many laser applications including ranging and remote sensing. The intracavity cell is also able to compensate optical aberrations from the resonator and from thermal effects in the active medium, resulting in near diffraction limited output [4], and eliminate the need for a conventional Q-switch as well, because its intensity-dependent reflectivity acts as a passive Q-switch, typically producing a train of nanosecond pulses of diffraction limited beam quality. One more significant use of OPC is a so-called short hologram, which does not exhibit in-depth diffraction deformation of the fine speckle pattern of the recording fields [5]. A thermal hologram in the output mirror was recorded by two speckle waves produced as a result of this recording a ring Nd:YAG laser [6]. Phase conjugation by SBS represents a fundamentally promising approach for achieving power scaling of solid-state lasers [7, 8] and optical fibers [9].

There are several theoretical models to describe OPC in resonators and lasers. One of them is to use the SBS reflection as one of the cavity mirrors of a laser resonator to form a so-called linear phase conjugate resonator [10], however ring-phase conjugate resonators are also possible [11]. The theoretical model of an OPC laser in transient operation [12] considers the temporal and spatial dynamic of the input field the Stokes field and the acoustic-wave amplitude in the SBS cell. On the other hand the spatial mode analysis of a laser may be carried out using transfer matrices, also know as ABCD matrices, which are a useful mathematical tool when studying the propagation of light rays through complex optical systems. They provide a simple way to obtain the final key characteristics (position and angle) of the ray. As an important example we could mention that transfer matrices have been used to study self-adaptive laser resonators where the laser oscillator is made out of a plane output coupler and an infinite nonlinear FWM medium in a self-intersecting loop geometry [13].

In this chapter we put forward an approach where the intracavity element is presented in the context of an iterative map (e.g. Tinkerbell, Duffing and Hénon) whose state is determined by its previous state. It is shown that the behavior of a beam within a ring optical resonator may be well described by a particular iterative map and the necessary conditions for its occurrence are discussed. In particular, it is shown that the introduction of a specific element within a ring phase-conjugated resonator may produce beams described by a Duffing, Tinkerbell or Hénon map, which we call "Tinkerbell, Duffing or Hénon beams". The idea of introducing map generating elements in optical resonators from a mathematical viewpoint was originally explored in [14-16] and this chapter is mainly based on those results.

This chapter is organized as follows: Section 2 discusses the matrix optics elements on which this work is based. Section 3 presents as an illustration some basic features of Tinkerbell, Duffing and Hénon maps, Sections 4,5 and 6 show, each one of them, the main characteristics of the map generation matrix and Tinkerbell, Duffing and Hénon Beams, as

well as the general case for each beams in a ring phase conjugated resonator. Finally Section 6 presents the conclusions.

2. ABCD matrix optics

Any optical element may be described by a 2×2 matrix in paraxial optics. Assuming cylindrical symmetry around the optical axis, and defining at a given position z both the perpendicular distance of any ray to the optical axis and its angle with the same axis as $y(z)$ and $\theta(z)$, when the ray undergoes a transformation as it travels through an optical system represented by the matrix $[A,B,C,D]$, the resultant values of y and θ are given by [17]:

$$\begin{pmatrix} y_{n+1} \\ \theta_{n+1} \end{pmatrix} = \begin{pmatrix} A & B \\ C & D \end{pmatrix} \begin{pmatrix} y_n \\ \theta_n \end{pmatrix}. \tag{1}$$

For any optical system, one may obtain the total $[A,B,C,D]$ matrix, by carrying out the matrix product of the matrices describing each one of the optical elements in the system.

2.1. Constant ABCD elements

For passive optical elements such as lenses, interfaces between two media, reflections, propagation, and many others, the elements A, B, C, D are constants and the determinant $\mathrm{Det}[A,B,C,D] = n_n/n_{n+1}$, where n_n and n_{n+1} are the refraction index before and after the optical element described by the matrix. Since typically n_n and n_{n+1} are the same, it holds that $\mathrm{Det}[A,B,C,D] = 1$.

2.2. Non constant ABCD elements

However, for active or non-linear optical elements the A, B, C, D matrix elements are not constant but may be functions of various parameters. The following three examples are worth mentioning.

2.2.1. Curved interface with a Kerr electro-optic material

Due to the electro-optic Kerr effect the refraction index of an optical media n is a function of the electric field strength E [18]. The change of the refraction index is given by $\Delta n = \lambda K E^2$, where λ is the wavelength and K is the Kerr constant of the media. For example, the $[A,B,C,D]$ matrix of a curved surface of radius of curvature r separating two regions of refractive index n_1 and n_2 (taking the center of the radius of curvature positive to the right in the zone of refractive index n_2) is given as:

$$\begin{pmatrix} 1 & 0 \\ -\dfrac{(n_2 - n_1)}{r} & 1 \end{pmatrix}. \tag{2}$$

Having vacuum ($n_1 = 1$) on the left of the interface and a Kerr electro-optic material on the right, the above [*ABCD*] matrix becomes

$$\begin{pmatrix} 1 & 0 \\ -\dfrac{(n_2(E)-1)}{r} & 1 \end{pmatrix}. \tag{3}$$

Clearly the elements *A, B, D* are constants but element *C* is a function of the electric field *E*.

2.2.2. Phase conjugate mirror

A second example is a phase conjugate mirror. The process of phase conjugation has the property of retracing an incoming ray along the same incident path [7]. The ideal ABCD phase conjugate matrix is

$$\begin{pmatrix} 1 & 0 \\ 0 & -1 \end{pmatrix}. \tag{4}$$

One may notice that the determinant of this particular matrix is not 1 but -1. The ABCD matrix of a real phase conjugated mirror must take into account the specific process to produce the phase conjugation. As already mentioned, typically phase conjugation is achieved in two ways; Four Wave Mixing or using a stimulated scattering process such as Brillouin, i.e. SBS. However upon reflection on a stimulated SBS phase conjugated mirror, the reflected wave has its frequency ω downshifted to $\omega - \delta = \omega(1 - \delta/\omega)$ where δ is the characteristic Brillouin downshift frequency of the mirror material (typically $\delta/\omega \ll 1$). In a non-ideal (i.e. real) case one must take the downshifting frequency into account and the ABCD matrix reads

$$\begin{pmatrix} 1-\dfrac{\delta}{\omega} & 0 \\ 0 & -1 \end{pmatrix}. \tag{5}$$

Furthermore, since in phase conjugation by SBS a light intensity threshold must be reached in order to have an exponential amplification of the scattered light, the above ideal matrix (4) must be modified. The scattered light intensity at position *z* in the medium is given as

$$I_S(z) = I_S(0)\exp(g_B I_L l), \tag{6}$$

where $I_S(0)$ is the initial level of scattering, g_B denotes the characteristic exponential gain coefficient of the scattering process, I_L is the intensity of the incident light beam, and *l* is the interaction length over which amplification takes place. Given the amplification $G = \exp(g_B(v)I_L l)$ the threshold gain factor is commonly taken as $G \sim \exp(30) \approx 10^{13}$ which corresponds to a threshold intensity

$$I_{L,th} = \frac{30}{g_B l}. \tag{7}$$

The modeling of a real stimulated Brillouin scattering phase conjugate mirror usually takes into account a Gaussian aperture of radius a at intensity $1/e^2$ placed before an ideal phase conjugator. In this way the reflected beam is Gaussian and only the parts of the Gaussian incident beam with intensity above threshold are phase conjugate reflected. The matrix of this aperture is given by:

$$\begin{pmatrix} 1 & 0 \\ -\dfrac{i\lambda}{\pi a^2} & 1 \end{pmatrix}, \tag{8}$$

where the aperture a is a function of the incident light intensity $a(I_L)$ (I_L must reach threshold to initiate the scattering process). As we can see, depending on the model, the *ABCD* matrix elements of a phase conjugated mirror may depend on several parameters such as the Brillouin downshifting frequency, the Gaussian aperture radius and the incident light intensity [19].

2.3. Systems with hysteresis

At last, as third example we may consider a system with hysteresis. It is well known that such systems exhibit memory. There are many examples of materials with electric, magnetic and elastic hysteresis, as well as systems in neuroscience, biology, electronics, energy and even economics which show hysteresis. As it is known in a system with no hysteresis, it is possible to predict the system's output at an instant in time given only its input at that instant in time. However in a system with hysteresis, this is not possible; there is no way to predict the output without knowing the system's previous state and there is no way to know the system's state without looking at the history of the input. This means that it is necessary to know the path that the input followed before it reached its current value. For an optical element with hysteresis the *ABCD* matrix elements are function of the y_n, y_{n-1}, …y_{n-i} and θ_n, θ_{n-1}, …, θ_{n-i} and its knowledge is necessary in order to find the state y_{n+1}, θ_{n+1}. In general, taking into account hysteresis, the [A,B,C,D] matrix of Eq. (1) may be written as:

$$\begin{pmatrix} A & B \\ C & D \end{pmatrix} = \begin{pmatrix} A\left(y_n, y_{n-1}, ...y_{n-i}, \theta_n, \theta_{n-1}, ...\theta_{n-i}\right) & B\left(y_n, y_{n-1}, ...y_{n-i}, \theta_n, \theta_{n-1}, ...\theta_{n-i}\right) \\ C\left(y_n, y_{n-1}, ...y_{n-i}, \theta_n, \theta_{n-1}, ...\theta_{n-i}\right) & D\left(y_n, y_{n-1}, ...y_{n-i}, \theta_n, \theta_{n-1}, ...\theta_{n-i}\right) \end{pmatrix}. \tag{9}$$

3. Dynamic maps

An extensive list of two-dimensional maps may be found in Ref. [20]. A few examples are Tinkerbell, Duffing and Hénon maps. As will be shown next they may be written as a matrix dynamical system such as the one described by Eq. (1) or equivalently as

$$y_{n+1} = Ay_n + B\theta_n, \quad (a)$$
$$\theta_{n+1} = Cy_n + D\theta_n. \quad (b)$$
(10)

3.1. Tinkerbell map

The Tinkerbell map [21, 22] is a discrete-time dynamical system given by the equations:

$$y_{n+1} = y_n^2 - \theta_n^2 + \alpha\, y_n + \beta\, \theta_n, (a)$$
$$\theta_{n+1} = 2y_n\theta_n + \gamma\, y_n + \delta\, \theta_n. \quad (b)$$
(11)

where y_n and θ_n are the scalar state variables and α, β, γ, and δ the map parameters. In order to write the Tinkerbell map as a matrix system such as Eq. (1) the following values for the coefficients A, B, C and D must hold:

$$A(y_n, \alpha) = y_n + \alpha,$$
(12)

$$B(\theta_n, \beta) = -\theta_n + \beta,$$
(13)

$$C(\theta_n, \gamma) = 2\theta_n + \gamma,$$
(14)

$$D(\delta) = \delta.$$
(15)

It should be noted that these coefficients are not constants but depend on the state variables y_n and θ_n and the Tinkerbell map parameters α, β, γ, and δ. Therefore as an *ABCD* matrix system the Tinkerbell map may be written as:

$$\begin{pmatrix} y_{n+1} \\ \theta_{n+1} \end{pmatrix} = \begin{pmatrix} y_n + \alpha & -\theta_n + \beta \\ 2\theta_n + \gamma & \delta \end{pmatrix} \begin{pmatrix} y_n \\ \theta_n \end{pmatrix}.$$
(16)

3.2. Hénon map

The Hénon map has been widely studied due to its nonlinear chaotic dynamics. Hénon map is a popular example of a two-dimensional quadratic mapping which produces a discrete-time system with chaotic behavior. The Hénon map is described by the following two difference equations [23, 24]:

$$y_{n+1} = 1 - \alpha y_n^2 + \theta_n, \quad (a)$$
$$\theta_{n+1} = \beta y_n. \quad (b)$$
(17)

Following similar steps as those of the Tinkerbell map, this map may be written as a dynamic matrix system:

$$\begin{pmatrix} y_{n+1} \\ \theta_{n+1} \end{pmatrix} = \begin{pmatrix} \dfrac{1}{y_n} - \alpha y_n & 1 \\ \beta & 0 \end{pmatrix} \begin{pmatrix} y_n \\ \theta_n \end{pmatrix} \tag{18}$$

where y_n and θ_n are the scalar state variables which can be measured as time series and α and β the map parameters. In many control systems α is a control parameter. The Jacobian β ($0 \leq \beta \leq 1$) is related to dissipation. The dynamics of the Hénon map is well studied (see, for instance, Ref. [25]) and its fixed points are given by:

$$(y_1, \theta_1) = \left(\frac{-\beta - 1 - \sqrt{(\beta+1)^2 + 4\alpha}}{2\alpha}, -\beta y_1 \right) \tag{19}$$

$$(y_2, \theta_2) = \left(\frac{-\beta - 1 + \sqrt{(\beta+1)^2 + 4\alpha}}{2\alpha}, -\beta y_2 \right). \tag{20}$$

And the corresponding eigenvalues are

$$\lambda_{1,2} = -\alpha y \pm \sqrt{(\alpha y)^2 - \beta}. \tag{21}$$

3.3. Duffing map

The study of the stability and chaos of the Duffing map has been the topic of many articles [26-27]. The Duffing map is a dynamical system which may be written as follows:

$$\begin{aligned} y_{n+1} &= \theta_n, & \text{(a)} \\ \theta_{n+1} &= -\beta y_n + \alpha \theta_n - \theta_n^3, & \text{(b)} \end{aligned} \tag{22}$$

where y_n and θ_n are the scalar state variables and α and β the map parameters. In order to write the Duffing map equations as a matrix system Eq. (1) the following values for the coefficients A, B, C and D must hold. It should be noted that these coefficients are not constants but depend on θ_n and the Duffing map parameters are as follows:

$$A = 0, \tag{23}$$

$$B = 1, \tag{24}$$

$$C(\beta) = -\beta, \tag{25}$$

$$D(\theta_n, \alpha) = \alpha - \theta_n^2. \tag{26}$$

Therefore as an ABCD matrix system the Duffing map may be written as:

$$\begin{pmatrix} y_{n+1} \\ \theta_{n+1} \end{pmatrix} = \begin{pmatrix} 0 & 1 \\ -\beta & \alpha - \theta_n^2 \end{pmatrix} \begin{pmatrix} y_n \\ \theta_n \end{pmatrix} \tag{27}$$

4. Maps in a ring phase-conjugated resonator

In this section an optical resonator with a specific map behavior for the variables y and θ is presented. Figure 1 shows a ring phase-conjugated resonator consisting of two ideal mirrors, an ideal phase conjugate mirror and a yet unknown optical element described by a matrix [a,b,c,e]. The two perfect plain mirrors [M] and the ideal phase conjugated mirror [PM] are separated by a distance d. The matrices involved in this resonator are: the identity matrix: $\begin{pmatrix} 1 & 0 \\ 0 & 1 \end{pmatrix}$ for the plane mirrors [M], $\begin{pmatrix} 1 & 0 \\ 0 & -1 \end{pmatrix}$ for the ideal phase conjugated mirror [PM], $\begin{pmatrix} 1 & d \\ 0 & 1 \end{pmatrix}$ for a distance d translation and, in addition, the unknown map generating device matrix represented by $\begin{pmatrix} a & b \\ c & e \end{pmatrix}$, is located between the plain mirrors [M] at distance $d/2$ from each one.
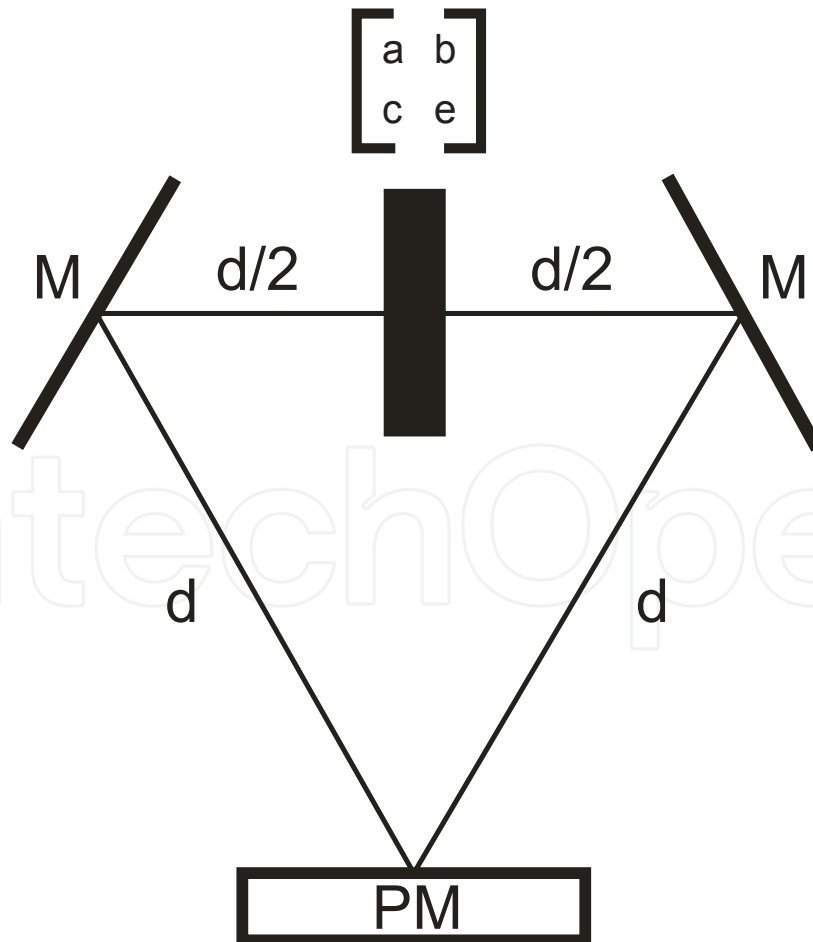
Figure 1. Ring phase conjugated laser resonator with chaos generating element.

For this system, the total transformation matrix [A,B,C,D] for a complete round trip is:

$$\begin{pmatrix} A & B \\ C & D \end{pmatrix} = \begin{pmatrix} 1 & 0 \\ 0 & -1 \end{pmatrix}\begin{pmatrix} 1 & d \\ 0 & 1 \end{pmatrix}\begin{pmatrix} 1 & 0 \\ 0 & 1 \end{pmatrix}\begin{pmatrix} 1 & d/2 \\ 0 & 1 \end{pmatrix}\begin{pmatrix} a & b \\ c & e \end{pmatrix}\begin{pmatrix} 1 & d/2 \\ 0 & 1 \end{pmatrix}\begin{pmatrix} 1 & 0 \\ 0 & 1 \end{pmatrix}\begin{pmatrix} 1 & d \\ 0 & 1 \end{pmatrix}.$$

(28)

The above one round trip total transformation matrix is

$$\begin{pmatrix} a + \dfrac{3cd}{2} & b + \dfrac{3d}{4}(2a + 3cd + 2e) \\ -c & -\dfrac{3cd}{2} - e \end{pmatrix}.$$

(29)

As can be seen, the elements of this matrix depend on the elements of the map generating matrix device [a,b,c,e]. If one does want a specific map to be reproduced by a ray in the ring optical resonator, then each round trip a ray described by (y_n, θ_n) has to be considered as an iteration of the desired map. Then, the *ABCD* matrix of the map system (16), (18), (27) must be equated to the total *ABCD* matrix of the resonator (29), this in order to generate a specific map dynamics for (y_n, θ_n).

It should be noticed that the results given by equations (28) and (29) are only valid for *b* small ($b \approx 0$). This is due to the fact that before and after the matrix element [a,b,c,e] we have a propagation of *d*/2. For a general case, expression (29) has to be substituted by:

$$\begin{pmatrix} A & B \\ C & D \end{pmatrix} = \begin{pmatrix} 1 & 0 \\ 0 & -1 \end{pmatrix}\begin{pmatrix} 1 & d \\ 0 & 1 \end{pmatrix}\begin{pmatrix} 1 & 0 \\ 0 & 1 \end{pmatrix}\begin{pmatrix} 1 & \dfrac{d-b}{2} \\ 0 & 1 \end{pmatrix}\begin{pmatrix} a & b \\ c & e \end{pmatrix}\begin{pmatrix} 1 & \dfrac{d-b}{2} \\ 0 & 1 \end{pmatrix}\begin{pmatrix} 1 & 0 \\ 0 & 1 \end{pmatrix}\begin{pmatrix} 1 & d \\ 0 & 1 \end{pmatrix}$$

(30)

Therefore the round trip total transformation matrix is:

$$\begin{pmatrix} a - \dfrac{c}{2}(b - 3d) & \dfrac{1}{4}\left[b^2 c - 2b\left(-2 + a + 3cd + e\right) + 3d\left(2a + 3cd + 2e\right)\right] \\ -c & \dfrac{1}{2}\left(bc - 3cd - 2e\right) \end{pmatrix}.$$

(31)

Matrix (29) describes a simplified ideal case whereas matrix (31) describes a general more complex and realistic case. These results will be widely used in the next three sections.

5. Tinkerbell beams

This section presents an optical resonator that produces beams following the Tinkerbell map dynamics; these beams will be called "Tinkerbell beams". Equation (29) is the one round trip total transformation matrix of the resonator. If one does want a particular map to be reproduced by a ray in the optical resonator, each round trip described by (y_n, θ_n), has to be considered as an iteration of the selected map. In order to obtain Tinkerbell beams, Eqs. (12) to (15) must be equated to Eq. (29), that is:

$$a + \frac{3cd}{2} = \alpha + y_n, \tag{32}$$

$$b + \frac{3d}{4}\left(2a + 3cd + 2e\right) = \beta - \theta_n, \tag{33}$$

$$c = -\gamma - 2\theta_n, \tag{34}$$

$$e + \frac{3cd}{2} = -\delta. \tag{35}$$

Equations (32-35) define a system for the matrix elements a, b, c, e, that guarantees a Tinkerbell map behaviour for a given ray (y_n, θ_n). These elements can be written in terms of the map parameters (α, β, γ and δ), the resonator's main parameter d and the ray state variables y_n and θ_n as:

$$a = \alpha + \frac{3}{2}\gamma d + 3d\theta_n + y_n, \tag{36}$$

$$b = \frac{1}{4}\left(4\beta - 6\alpha d + 6\delta d - 9\gamma d^2 - 4\theta_n - 18d^2\theta_n - 6dy_n\right), \tag{37}$$

$$c = -2\theta_n - \gamma, \tag{38}$$

$$e = -\delta + \frac{3}{2}d\left(\gamma + 2\theta_n\right). \tag{39}$$

The introduction of the above values for the $\begin{pmatrix} a & b \\ c & e \end{pmatrix}$ matrix in Eq. (28) enables us to obtain Eq. (16). For any transfer matrix elements A and D describe the lateral magnification while C describe the focal length, whereas the device's optical thickness is given by $B = L/n$, where L is its length and n its refractive index. From Eqs. (36-39) it must be noted that the upper elements (a and b) of the device matrix depend on both state variables (y_n and θ_n) while the lower elements (c and e) only on the state variable θ_n. The study of the stability and chaos of the Tinkerbell map in terms of its parameters is a well-known topic [21,22]. The behaviour of element b is quite interesting; figure 2 shows a computer calculation for the first 100 round trips of matrix element b of the Tinkerbell map generating device for a resonator of unitary length ($d = 1$) and map parameters $\alpha = 0$, $\beta = -0.6$, $\gamma = 0$ and $\delta = -1$, these parameters were found using brute force calculations and they were selected due to the matrix-element b behaviour (i.e. we were looking for behaviour able to be achievable in experiments). As can be seen, the optical length of the map generating device varies on each round trip in a periodic form, this would require that the physical length of the device, its refractive index - or a combination of both- change in time. The actual design of a physical Tinkerbell map generating device for a unitary ring resonator must satisfy Eqs. (36-39), to do so its elements (a, b, c and e) must vary accordingly.
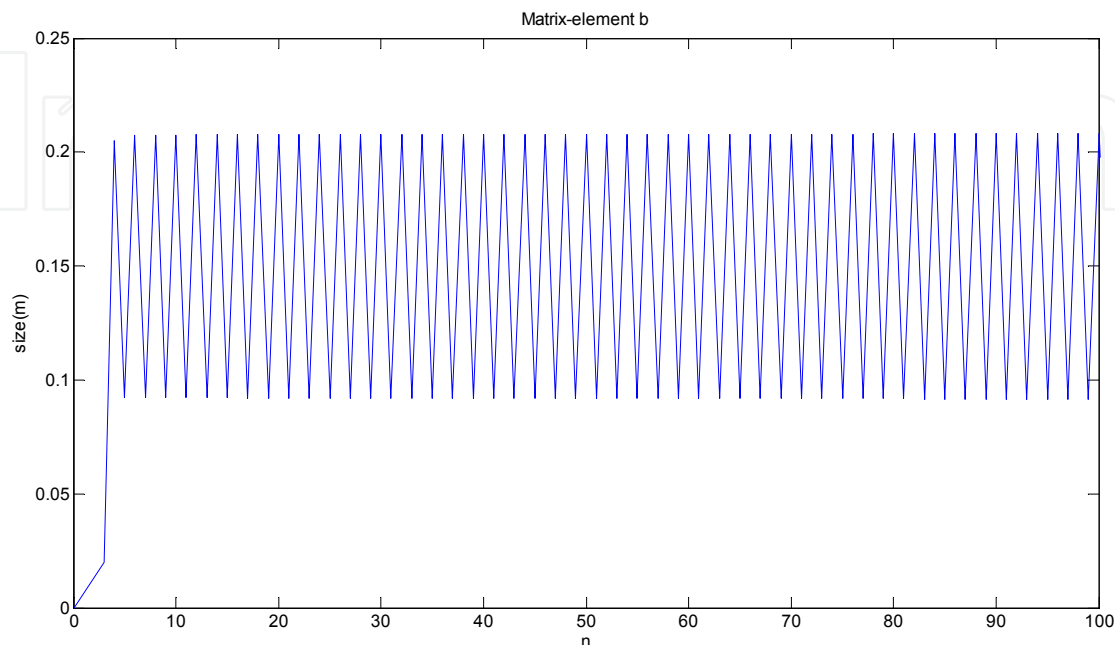
Figure 2. Computer calculation of the magnitude of matrix element b of the Tinkerbell map generating device for a resonator with $d = 1$ and Tinkerbell parameters $\alpha = 0$, $\beta = -0.6$, $\gamma = 0$ and $\delta = -1$ for the first 100 round trips.

5.1. Tinkerbell beams: General case

To obtain the Eqs. (36-39) b, the thickness of the Tinkerbell generating device, has to be very small (close to zero), so the translations before and after the device can be over the same distance $d/2$. In the previous numeric simulation b takes values up to 0.2, so the general case where the map generating element b does not have to be small must be studied. As previously explained Eq. (28) must be substituted by Eq. (30).

From Eqs. (16) and (31) we obtain the following system of equations for the matrix elements a, b, c and e:

$$a - \frac{c}{2}(b - 3d) = \alpha + y_n, \tag{40}$$

$$\frac{1}{4}(b^2 c - 2b(-2 + a + 3cd + e) + 3d(2a + 3cd + 2e)) = \beta - \theta_n, \tag{41}$$

$$-c = \gamma + 2\theta_n, \tag{42}$$

$$\frac{bc - 3cd - 2e}{2} = \delta. \tag{43}$$

The solution to this new system is written as:

$$a = \alpha + \frac{3}{2}\gamma d + 3d\theta_n + y_n + \frac{1}{2\gamma + 4\theta_n}\left(\begin{array}{c}\gamma\left(2 - \alpha + \delta - 3\gamma d - 12d\theta_n - y_n\right)\\ +\theta_n\left(4 - 2\alpha + 2\delta - 12d\theta_n - 2y_n\right)\\ -\left(-\dfrac{\gamma}{2} - \theta_n\right)\sqrt{P^2 - Q}\end{array}\right), \tag{44}$$

$$b = \frac{1}{\gamma + 2\theta_n}\left(-2 + \alpha - \delta + 3\gamma d + 6d\theta_n + y_n + \frac{\sqrt{P^2 - Q}}{2}\right), \tag{45}$$

$$c = -\gamma - 2\theta_n, \tag{46}$$

$$e = \delta + \frac{3}{2}\gamma d + 3d\theta_n + \frac{1}{2\gamma + 4\theta_n}\left(\begin{array}{c}\gamma\left(2 - \alpha + \delta - 3\gamma d - 12d\theta_n - y_n\right)\\ +\theta_n\left(4 - 2\alpha + 2\delta - 12d\theta_n - 2y_n\right)\\ -\left(-\dfrac{\gamma}{2} - \theta_n\right)\sqrt{P^2 - Q}\end{array}\right), \tag{47}$$

where:

$$P = 4 - 2\alpha + 2\delta - 6\gamma d - 12d\theta_n - 2y_n$$

and

$$Q = \left(4\gamma + 8\theta_n\right)\left(-4\beta + 6\gamma d - 6\delta d + 9\gamma d^2 + 4\theta_n + 18d^2\theta_n + 6dy_n\right).$$

It should be noted that if one takes into account the thickness of the map generating element, the equations complexity is substantially increased. Now only c has a simple relation with θ_n and γ, on the other hand a, b and e are dependent on both state variables, on all Tinkerbell parameters, as well as on the resonator length. When the calculation is performed for this new matrix with the following map parameters: $\alpha = 0.4$, $\beta = -0.4$, $\gamma = -0.3$ and $\delta = 0.225$, figure 3 is obtained. The behaviour observed in figure 3 for the matrix-element b can be obtained for several different parameters' combinations, as well as other dynamical regimes with a lack of relevance to our work. One can note that after a few iterations the device's optical thickness is small and constant, this should make easier a physical implementation of this device.
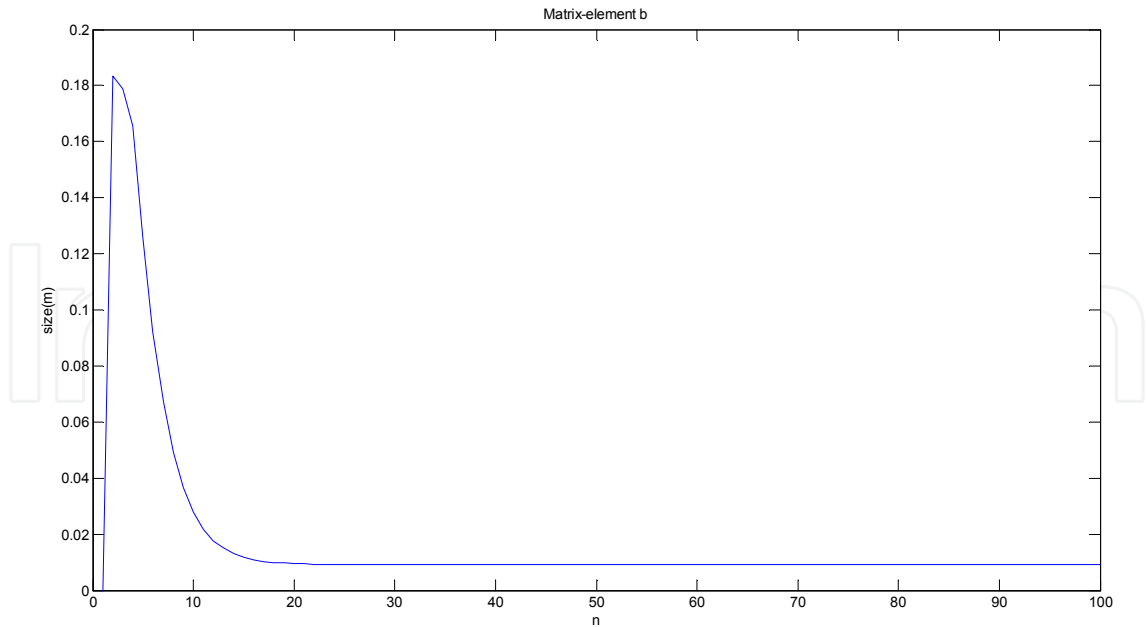
Figure 3. Computer calculation of the magnitude of matrix element b of the Tinkerbell map generating device for a resonator with $d = 1$ and Tinkerbell parameters $\alpha = 0.4$, $\beta = -0.4$, $\gamma = -0.3$ and $\delta = 0.225$ for the first 100 round trips.

6. Duffing beams

This section presents an optical resonator that produces beams following the Duffing map dynamics; these beams will be called "Duffing beams". Equation (29) is the one round trip total transformation matrix of the resonator. If one does want a particular map to be reproduced by a ray in the optical resonator, each round trip described by (y_n, θ_n), has to be considered as an iteration of the selected map. In order to obtain Duffing beams, Eqs. (23) to (26) must be equated to Eq. (29), that is:

$$a + \frac{3cd}{2} = 0, \tag{48}$$

$$b + \frac{3d}{4}\left(2a + 3cd + 2e\right) = 1, \tag{49}$$

$$-c = -\beta, \tag{50}$$

$$-\frac{3cd}{2} - e = \alpha - \theta_n^2. \tag{51}$$

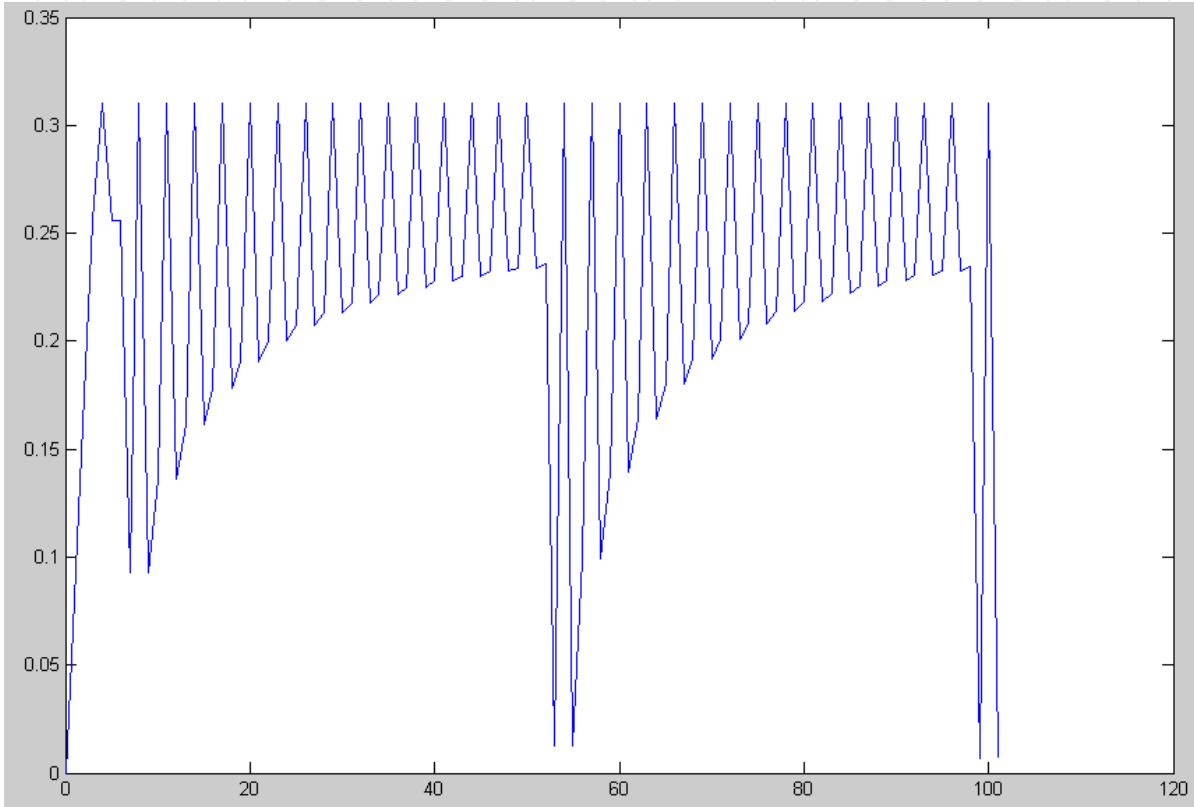Equations (48-51) define a system for the matrix elements of a, b, c, e, enabling the generation of a Duffing map for the y_n and θ_n state variables. Its solution is:

$$a = -\frac{3\beta d}{2}, \tag{52}$$

$$b = \frac{1}{4}\left(4 + 6\alpha d + 9\beta d^2 - 6d\theta_n^2\right),$$ (53)

$$c = \beta,$$ (54)

$$e = -\alpha - \frac{3d\beta}{2} + \theta_n^2.$$ (55)

Figure 4. Computer calculation of the magnitude of matrix element b of the Duffing map generating device for a resonator with $d = 1$ and Duffing parameters $\alpha = 1.04$ and $\beta = -1$ for the first 100 round trips.

As can be seen these matrix elements depend on the Duffing parameters α and β as well as on the resonator main parameter d and on the state variable θ_n. These are the values which must be substituted for the $[a,b,c,e]$ matrix in equation (28) for the round trip matrix. As expected, the introduction of the above $[a,b,c,e]$ matrix elements in Eq. (29) produces the *ABCD* matrix of the Duffing Map, Eq. (27). For a general *ABCD* transfer matrix, elements A and D are related to the lateral magnification and element C to the focal length, whereas element B gives the optical length of the device. The optical thickness of the *ABCD* is; $B = L/n$, where L is the physical length of the device and n its refractive index. From Eqs. (52-55) we may see that the A and C elements of the matrix $[a,b,c,e]$ are constants depending only on the resonator parameter d and the Duffing parameters α and β. However matrix elements B and D are dynamic ones and depend on the state variable θ_n. Of special interest is element B of the map generating matrix $[a,b,c,e]$. Figure 4 shows a computer calculation of matrix element B of the Duffing map generating device for a resonator with $d = 1$ and Duffing

parameters α = 1.04 and β = -1 for the first 100 round trips. As it is well known, depending on the α and β map parameters different dynamic states may be obtained including chaos. As can be seen the optical length of the map generating device given by the B matrix element varies on each round trip. This requires that either the physical length of the device or its refractive index, or a combination of both, changes as shown in Figure 4. The design of a physical Duffing map generating device for this resonator must satisfy Eqs. (52-55). A physical implementation of this device is possible as long as its $ABCD$ elements vary according to these equations.

6.1. Duffing beams: General case

The results given by Eqs. (52-55) are valid only when the b element of the $[a,b,c,e]$ matrix is small. As can be seen from Eq. (28), the thickness of the Duffing map generating element (described by matrix $[a,b,c,e]$) must be close to zero. This because in Eq. (28) the matrix before and after the $[a,b,c,e]$ is a matrix for a $d/2$ translation which is possible only if $b = 0$ or very small. The previous numeric simulation shows that the b element takes the values of up to 0.3. Therefore one must consider a general case where the map generating element b has not the limitation of being asked to be small. For a general case, Eq. (28) must be substituted by Eq. (30) and (31). From expressions (27) and (31) we obtain the following system of equations for the matrix elements a, b, c, e:

$$a - \frac{c}{2}(b - 3d) = 0, \tag{56}$$

$$\frac{1}{4}(b^2 c - 2b(-2 + a + 3cd + e) + 3d(2a + 3cd + 2e)) = 1, \tag{57}$$

$$-c = -\beta, \tag{58}$$

$$\frac{bc - 3cd - 2e}{2} = \alpha - \theta_n^2. \tag{59}$$

The solution to this system is given by:

$$a = \frac{2 + \alpha - \theta_n^2 + \sqrt{\alpha^2 + 4\beta(-1 + 3d) - 2\alpha(-2 + \theta_n^2) + (-2 + \theta_n^2)^2}}{2}, \tag{60}$$

$$b = \frac{2 + \alpha + 3\beta d - \theta_n^2 + \sqrt{\alpha^2 + 4\beta(-1 + 3d) - 2\alpha(-2 + \theta_n^2) + (-2 + \theta_n^2)^2}}{\beta}, \tag{61}$$

$$c = \beta, \tag{62}$$

$$e = \frac{2 - \alpha + \theta_n^2 + \sqrt{\alpha^2 + 4\beta(-1 + 3d) - 2\alpha(-2 + \theta_n^2) + (-2 + \theta_n^2)^2}}{2}. \tag{63}$$

As we may see, taking into account the thickness of the map generating element device described by matrix $[a,b,c,e]$ greatly increases its complexity. Now only the C matrix element is constant, being elements A, B and D dependent on the state variable θ_n and on the Duffing parameters α and β as well as on the resonator main parameter d. Figure 5 shows a computer calculation of the matrix element B of the Duffing map generating device for a resonator with $d = 1$ and Duffing parameters $\alpha = 1.04$ and $\beta = -0.6$ for the first 100 round trips. As can be seen, the optical thickness variation of the map generating device now is rather small, which means that the length and/or refractive index variation of the map generating element is also small and favors a physical realization of this device.
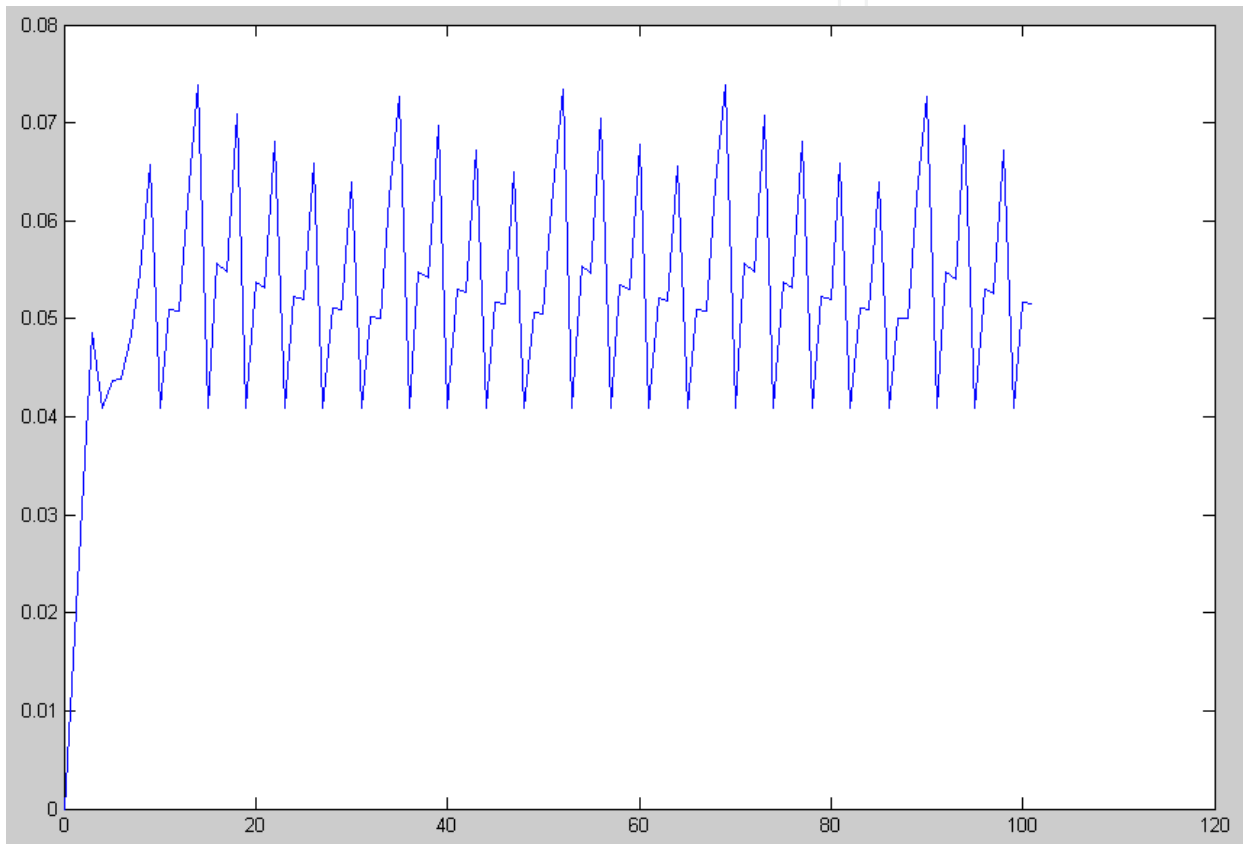
Figure 5. Computer calculation of the magnitude of matrix element b of the Duffing map generating device for a resonator with $d = 1$ and Duffing parameters $\alpha = 1.04$ and $\beta = -0.6$ for the first 100 round trips.

7. Hénon beams

This section presents an optical resonator that produces beams following the Hénon map dynamics; these beams will be called "Hénon beams". Equation (29) is the one round trip total transformation matrix of the resonator. If one does want a particular map to be reproduced by a ray in the optical resonator, each round trip described by (y_n, θ_n), has to be considered as an iteration of the selected map. In order to obtain Hénon beams, the $[A, B, C, D]$ elements of Eq. (18) must be equated to Eq. (29), that is:

$$a + \frac{3cd}{2} = \frac{1}{y_n} - \alpha y_n, \tag{64}$$

$$b + \frac{3d}{4}\left(2a + 3cd + 2e\right) = 1, \tag{65}$$

$$-c = \beta, \tag{66}$$

$$-\frac{3cd}{2} - e = 0. \tag{67}$$

The solution for the Hénon chaos matrix elements [a,b,c,e], able to produce Hénon beams in terms of the Hénon Map are the following:

$$a = \frac{3\beta d}{2} + \frac{1}{y_n} - \alpha y_n, \tag{68}$$

$$b = 1 + \frac{3}{2}d\left(-\frac{1}{y_n} + \alpha y_n - \frac{3d\beta}{2}\right), \tag{69}$$

$$c = -\beta, \tag{70}$$

$$e = \frac{3d\beta}{2}. \tag{71}$$

As can be seen the matrix elements depend on the Hénon parameters α and β as well as on the resonator main parameter d and on the state variable y_n. However when analyzing the behavior of element "b" (Eq. (69)) we may see that there is a problem caused by the term $1/y_n$. While for the case of Tinkerbell and Duffing beams we were able to look at the behavior of the obtained "b" element for small values of y_n, as it is shown in figures (2-5), this is not possible for the Henon case because small values of y_n will produce very large values for "b", therefore making very difficult to obtain solutions with practical value.

7.1. Hénon beams: General case

In an analogous way to the two previous cases, using expression (18) and (31) we obtain for the general Hénon chaos matrix elements [a,b,c,e]:

$$a = \frac{-1 - 2y_n + \alpha y_n^2 + \sqrt{1 - 4y_n - 2\left(-2 + \alpha - 2\beta + 6\beta d\right)y_n^2 + 4\alpha y_n^3 + \alpha^2 y_n^4}}{2y_n}, \tag{72}$$

$$b = \frac{1 + \left(-2 + 3\beta d\right)y_n - \alpha y_n^2 + \sqrt{1 - 4y_n - 2\left(-2 + \alpha - 2\beta + 6\beta d\right)y_n^2 + 4\alpha y_n^3 + \alpha^2 y_n^4}}{2y_n}, \tag{73}$$

$$c = -\beta, \tag{74}$$

$$e = \frac{-1 + 2y_n + \alpha y_n^2 - \sqrt{1 - 4y_n - 2(-2 + \alpha - 2\beta + 6\beta d)y_n^2 + 4\alpha y_n^3 + \alpha^2 + y_n^4}}{2y_n}. \tag{75}$$

8. Conclusions

This chapter presents a description of the application of non-constant ABCD matrix in the description of ring optical phase conjugated resonators. It is shown how the introduction of a particular map generating device in a ring optical phase-conjugated resonator can generate beams with the behavior of a specific two dimensional map. In this way beams that behave according to the Tinkerbell, Duffing or Henon Maps which we call "Tinkerbell, Duffing or Henon Beams", are obtained.

In particular, this chapter shows how Tinkerbell beams can be produced if a particular device is introduced in a ring optical phase-conjugated resonator. The difference equations of the Tinkerbell map are explicitly introduced in an *ABCD* transfer matrix to control the beams behaviour. The matrix elements *a*, *b*, *c* and *e* of a map generating device are found in terms of the map parameters (α, β, γ and δ), the state variables (y_n and θ_n) and the resonator length. The mathematical characteristics of an optical device inside an optical resonator capable to produce Tinkerbell beams are found. In the general case a device with fixed size was obtained, opening the possibility of a continuance of this work; that is the actual building of an optical device with these *a*, *b*, *c* and *d* matrix elements according to the description given and the experimental observation of Tinkerbell beams.

Also, it is explicitly shown how the difference equations of the Duffing map can be used to describe the dynamic behavior of what we call Duffing beams i.e. beams that behave according to the Duffing map. The matrix elements *a*, *b*, *c*, *e* of a map generating device are found in terms of α and β, the Duffing parameters, the state variable θ_n and the resonator parameter *d*.

Finally it is shown that the difference equations of the Hénon map can be used to describe the dynamical behavior of Hénon beams. The matrix elements *a, b, c, e* of a chaos generating device are found in terms of α and β the Hénon parameters, and *d* the resonator parameter.

Author details

V. Aboites[*], Y. Barmenkov and A. Kir'yanov
Centro de Investigaciones en Óptica, México

M. Wilson
Université des Sciences et Technologies de Lille, France

---

[*] Corresponding Author

9. References

[1] G.S. He, Optical Phase Conjugation: Principles, Techniques and Applications, Progress in Quantum Electronics 26, No, 3, (2002), 61p.

[2] H.-J. Eichler, R. Menzel, and D. Schumann, Appl. Opt., 31 No. 24 (1992) 5038-5043

[3] M. O'Connor, V. Devrelis, and J. Munch, in Proc. Int. Conf. on Lasers'95 (1995) pp. 500-504

[4] M. Ostermeyer, A. Heuer, V. Watermann, and R. Menzel in Int. Quantum Electronics Conf., 1996 OSA Technical Digest Series (Optical Society of America, Washington, DC, 1996), p. 259

[5] Bel'dyugin I.M., Galushkin M.G., and Zemskov E.M. Kvantovaya Elektron., 11, 887 (1984) [Sov. J. Quantum Electron., 14, 602 (1984); Bespalov V.I. and Betin A.A. Izv. Akad. Nauk SSSR., Ser. Fiz., 53 1496 (1989)

[6] V.V. Yarovoi, A.V. Kirsanov, Phase conjugation of speckle-inhomogeneous radiation in a holographic Nd:YAG laser with a short thermal hologram, Quantum Electronics 32(8) 697-702 (2002)

[7] M.J. Damzen, V.I. Vlad, V. Babin, and A. Mocofanescu, Stimulated Brillouin Scattering: Fundamentals and Applications, Institute of Physics, Bristol (2003)

[8] D. A. Rockwell, A review of phase-conjugate solid-state lasers, IEEE Journal of Quantum Electronics 24, No. 6, (1988) 1124-1140

[9] Dämmig, M., Zinner, G., Mitschke, F., Welling, H. Stimulated Brillouin scattering in fibers with and without external feedback (1993) Physical Review A, 48 (4), pp. 3301-3309

[10] P.J. Soan, M.J. Damzen, V. Aboites and M.H.R. Hutchinson, Opt. Lett. 19 (1994), 783

[11] A.D. Case, P.J. Soan, M.J. Damzen and M.H.R. Hutchinson, J. Opt. Soc. Am. B 9 (1992) 374

[12] B. Barrientos, V. Aboites, and M. Damzen, Temporal dynamics of a ring dye laser with a stimulated Brillouin scattering mirror, Applied Optics, 35 (27) 5386-5391 (1996)

[13] E. Rosas, V. Aboites, M.J. Damzen, FWM interaction transfer matrix for self-adaptive laser oscillators, Optics Communications 174 243-247 (2000)

[14] V. Aboites, Int. J. of Pure and Applied Mathematics, 36, No. 4 (2007) 345-352.

[15] V. Aboites and M. Wilson, Int. J. of Pure and Applied Mathematics, 54 No. 3 (2009) 429-435.

[16] V. Aboites, A.N. Pisarchik, A. Kiryanov, X. Gomez-Mont, Opt. Comm., 283, (2010) 3328-3333

[17] A. Gerrard and J.M. Burch, Introduction to Matrix Methods in Optics, Dover Publications Inc., New York (1994).

[18] Y. Hisakado, H. Kikuchi, T. Nagamura, and T. Kajiyama, Advanced Materials, 17 No.1 (2005) 96-97

[19] A.V. Kir'yanov, V. Aboites and N.N. Il'ichev, JOSA B, 17 (2000) 11-17

[20] http://en.wikipedia.org/wiki/List_of_chaotic_maps

[21] R.L. Davidchack, Y.C. Lai, A.Klebanoff, E.M. Bollt, Physics Letters A, 287 (2001) 99-104

[22] P.E. McSharry, P.R.C. Ruffino, Dynamical Systems, 18, No. 3 (2003) 191-200

[23] E. Eschenazi, H.G. Solari, and R. Gilmore, Phys. Rev. A 39 (1989) 2609.

[24] M. Hénon, Commun. Math. Phys. 50 (1976) 69.

[25] R.L. Devaney, An Introduction to Chaotic Dynamical Systems, Addison-Wesley, Redwood City (1989).

[26] L.M. Saha and R. Tehri, Int. J. of Appl. Math and Mech., 6 (1) (2010) 86-93

[27] C. Murakami, W. Murakami, K. Hirose and W.H. Ichikawa, Chaos, Solitons & Fractals, 16 (2) (2003) 233-244